



# Morphology, optical and scintillation properties of $\text{Eu}^{2+}$ -sensitized CsI(Na) thick film

Elham Khodadoost\*, M.E. Azim Araghi

Applied Physics Division, Physics Department, Kharazmi University, 43 Mofateh Avenue, Tehran, Iran

## ARTICLE INFO

### Keywords:

CsI(Na)  
Eu co-doping  
Luminescence  
High quantum efficiency  
Energy transfer  
Scintillator

## ABSTRACT

Europium and Sodium co-doped CsI and CsI(Na) thick films are deposited by thermal evaporation on the quartz substrate coated with a nano-reflective layer. The morphology and crystal structure of the deposited films, using the SEM images and the X-ray diffraction patterns, exhibited no distinguishable differences. Inductively coupled plasma optical emission spectroscopy ICP (OES) was utilized to measure sodium and europium concentrations in the deposition. Moreover, their optical properties were investigated by UV absorption, excitation, and emission spectroscopy in the wavelength region of 200–800 nm. The results indicated that Eu-sensitizing material enhanced the absorption and photoluminescence intensity of the CsI(Na) columnar-structure film compared to that of conventional CsI(Na) scintillator. This increase was attributed to both the Eu's high quantum efficiency and the energy transfer between the activator and sensitizer. Ion beam-induced luminescence (IBIL) measurements also confirmed the photoluminescence results. Gamma rays spectroscopy testified to the improvement of CsI(Na, Eu) scintillation efficiency in comparison with the traditional CsI(Na) scintillator.

## 1. Introduction

CsI(Na) is a remarkably efficient scintillation material that has been widely investigated and used for decades. In almost all physical parameters, it is identical to CsI(Tl) and possesses its favorable characteristic of not cleaving and being relatively soft and machinable. From the scintillation standpoint, CsI(Na) has the highest light output next to the thallium-doped NaI. The light output is comfortably into the blue region of the spectrum and there are no significant problems with self-absorption of the scintillation light. It has a higher mass attenuation coefficient than NaI(Tl) and high  $\gamma$  and X-ray stopping power of host lattice from relatively high physical density ( $4.53 \text{ g/cm}^3$ ) and high atomic number [1–5]. It plays an important role, as scintillation counters, in the formation of the films [6–9]. CsI(Na) bulk crystal has an efficient blue luminescence, which has been studied by two approaches. The first approach is self-trapped exciton (STE) of pure CsI crystal perturbed by the possible effects of  $\text{Na}^+$  ion, and the other is energy transfer from the CsI host material to Na nanoparticles [4,10].

Most current scintillators suffer from poor scintillation properties which limit the accuracy of their functional capacity. Therefore, it is more desirable to either invent new scintillator or improve the scintillation properties of existing ones or both. It has recently been found that co-doping of traditional scintillation materials can improve their properties [11–14]. To the best of our knowledge, there is no published work on sensitized CsI(Na). In this research, the feasibility of modifying scintillation properties in CsI(Na) scintillator material by

co-doping with  $\text{Eu}^{2+}$  is deduced from Eu high quantum efficiency due to  $4f^6 5d \rightarrow 4f^7$  transitions [13,15]. As the literature indicates [16–18], CsI(Eu), for excitation at 240 nm, has a weak broad emission band (around 410–480 nm) at room temperature (RT), which is intensified in the region of 441–448 nm at low temperature. The Eu-doped CsI scintillator could not be an efficient scintillator at RT since a small Stokes shift, self-absorption, and scintillator efficiency loss; however, as a co-dopant, it increases the luminescence intensity [19].

In this research, we study Eu and Na co-doped CsI crystals as a sensitizer in the form of thick films by using the physical vapor deposition (PVD) method. The deposited film properties are characterized morphologically by using the SEM and XRD analyses, and then, optically by ICP (OES), UV absorption, excitation, photoluminescence and IBIL. The response to  $^{137}\text{Cs}$  gamma rays is studied in order to obtain their scintillation light yield.

## 2. Experimental

### 2.1. Preparing thick films

The quartz substrates in the dimensions of  $1'' \times 1'' \times 0.04''$ , were coated by different thin layers (50 nm- $\text{TiO}_2$ , 50 nm-Al, 50 nm-Ag), using electron beam gun evaporation to provide the best reflective layers through UV-Vis analysis. Then, the films were deposited by thermal evaporation in the vacuum ( $10^{-5}$  torr) and the reactive atmosphere

\* Corresponding author.

E-mail address: [Std\\_elkhodadoost@khu.ac.ir](mailto:Std_elkhodadoost@khu.ac.ir) (E. Khodadoost).

to prevent O<sub>2</sub> contamination. The general process utility of this kind of deposition has been commonly used for decades [20]. The crushed CsI(Na) and CsI(Na, Eu) single crystals were used as raw materials. The optimal concentration of Na activator was 0.02% mol and the intended amount of Eu sensitizer was about 0.001% mol, by referring to the literature [13,21]. The heat treatment was performed at 250 °C for 20 min.

## 2.2. Characterization

Inductively coupled plasma-optical emission spectroscopy (ICP-OES; Model 730-ES, Varian), in the wavelength region of 167–785 nm, with CCD detector, was used to detect Na and Eu concentration, in the films. The instrument detection limit was 1 ppb. All the films were dissolved in deionized water.

The crystal structure of the samples was characterized by X-ray diffractometer (XRD; Model Panalytical Company X'Pert PRO MPD) at the  $2\theta$  range of 5–90°. The surface morphology was observed using a scanning electron microscopy (SEM; Model Tescan—Mira III). The UV-Vis analysis was performed using Perkin-Elmer UV-Vis spectrometer. Photoluminescence and UV-excitation spectra were recorded in the wavelength region of 200–800 nm, in the Varian Cary Eclipse model at RT.

Ion beam induced luminescence (IBIL) measurement was performed using the micro beam facility of the Van de Graff Laboratory (Tehran, Iran) and based on an Oxford micro beam triplet setup. This instrument has a proton beam of 2.5 MeV and ~100 pA current, with a spot size of 10×10 μm<sup>2</sup> on the sample surface. For each measurement, an area of 1×1 mm<sup>2</sup> was scanned for 30 min. The system was set on a collimating lens of 2.3 cm focal length at 135° to the beam direction, which was used to guide the IBIL to the outside of the reaction chamber. A fiber optic (with 400 μm diameter) was connected to the collimating lens for collecting the sample luminescence and transmitting it to the spectrometer. In order to collect the IBIL spectra of samples within the desired area, the beam was well focused on a spot size and spectra were recorded for 1 min. IBIL measurements of the samples were carried out at RT condition. The IBIL images of samples were captured through an OPTIKA PRO 5 CCD.

The pulse height spectrum of CsI(Na) and CsI(Na, Eu) thick films was obtained under excitation with 662 keV gamma rays from a <sup>137</sup>Cs source (20 μCi). The film coated surface was optically coupled to a photomultiplier tube using silicone grease. The film surface's other side was covered by Teflon reflective layer. Nano coated layer, Teflon layer and silicone grease layer were used to reflect scintillation photons back in to the sample, to improve the scintillation efficiency, this consideration is photon management. The source was located along the cylindrical axis of the scintillator and a photomultiplier (PMT; Model FEU 31, Russia) at a 10 cm distance from the surface of the sample crystal. Nuclear electronic system consisted of a high voltage supply (CC228 01Y BEIJING Hamamatsu, China), preamplifier (IAP 3001 Iran), amplifier (IAP 3600 Iran), MCA (a HVMCA NT-124), and a data acquisition system. NTMCA software was used to analyze the integrated spectrum. To ensure the results, all measurements were repeated twice under the same conditions by using the same thick films.

## 3. Results and discussion

### 3.1. UV-reflection

TiO<sub>2</sub>, Al, and Ag crystals were used to coat onto the quartz substrate through electron beam gun evaporation. These reflective layers were chosen because of their high reflectance. The external reflective nanolayers were used to reflect scintillation photon back in to the layers which improve the scintillation efficiency [22].

According to Fig. 1, by measuring the UV-reflection intensity, TiO<sub>2</sub> had a better response and hence was chosen in this research.

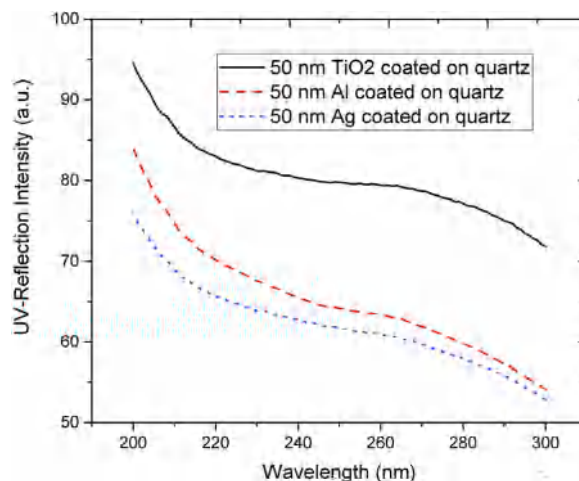


Fig. 1. UV-reflection intensity of TiO<sub>2</sub>, Al and Ag coated layers on quartz substrate.

### 3.2. Morphology and structure

The surface morphology of the deposited films was studied by scanning electron microscopy (SEM) as depicted in Fig. 2. CsI(Na) and CsI(Na, Eu) films seemed to have a column structure that can be appropriate to capture light. The columns' thickness was estimated to be about 500 μm and their diameter was about 3–10 μm, as seen in SEM images. So, according to Section 2.1, the size of thick films is almost the same, i.e. 1''×1''×500 μm.

As mentioned above, films were made of the CsI(Na) and CsI(Na, Eu) crushed single crystals. When deposition occurred, the column-structure crystals were formed—i.e. the evaporated crystals grew in a vertical direction in the deposited layers. As reported for the other alkali halide films like CsI(Eu) and CsI(Tl) [16,23–25], it is seen that no any defects like as displacement, impurity, or inclusion have no impact on the formation of the column structure. As seen in Fig. 2, the sample morphology has no distinguishable differences as the sensitizer was added.

It should be noted that the crystal quality of the host material (CsI) is not changed by adding the activator and sensitizer. Measuring X-ray diffraction patterns can verify this claim (Fig. 3). The diffraction peaks observed at  $2\theta$  of 39.473° and 84.895° are related to the (100) and (200) diffractions of CsI crystals. It is also observed that the preferred growth has been occurred along (100) direction. By doping Na and Eu into CsI, it was found that X-ray diffraction patterns are not changed, as illustrated in Fig. 3, which can be related to the very low amounts of activator and sensitizer.

ICP (OES) was used to confirm the existence of Na and Eu in the composition of the deposited films. The ICP data indicated that Na and Eu concentrations remain close compared to that of the crystal.

### 3.3. Excitation and absorption

As shown in Fig. 4, for emission at 430 nm, the excitation spectrum has two regions of 230–275 nm and 370–400 nm at RT. The excitation peak wavelengths of CsI(Na, Eu) are at 232 nm and 380 nm, and for CsI(Na) are at 240 nm and 373 nm. CsI(Na) excitation bands can be formed, using several configurations of various defect positions [2].

The absorption spectra of CsI(Na) and CsI(Na, Eu) films are shown in Fig. 5. For CsI(Na), there are two absorption bands in the range of 2.95–3.35 eV and from 3.75 to 5.5 eV, while for CsI(Na, Eu), there are three absorption bands in the range of 2.95–3.35 eV then around 4 eV and from 4.75 to 5.5 eV. It is deduced that by adding Eu as a sensitizer to CsI(Na), the new absorption sub-levels due to 4f → 5d transitions [18] were created which overlap with CsI(Na) absorption levels.

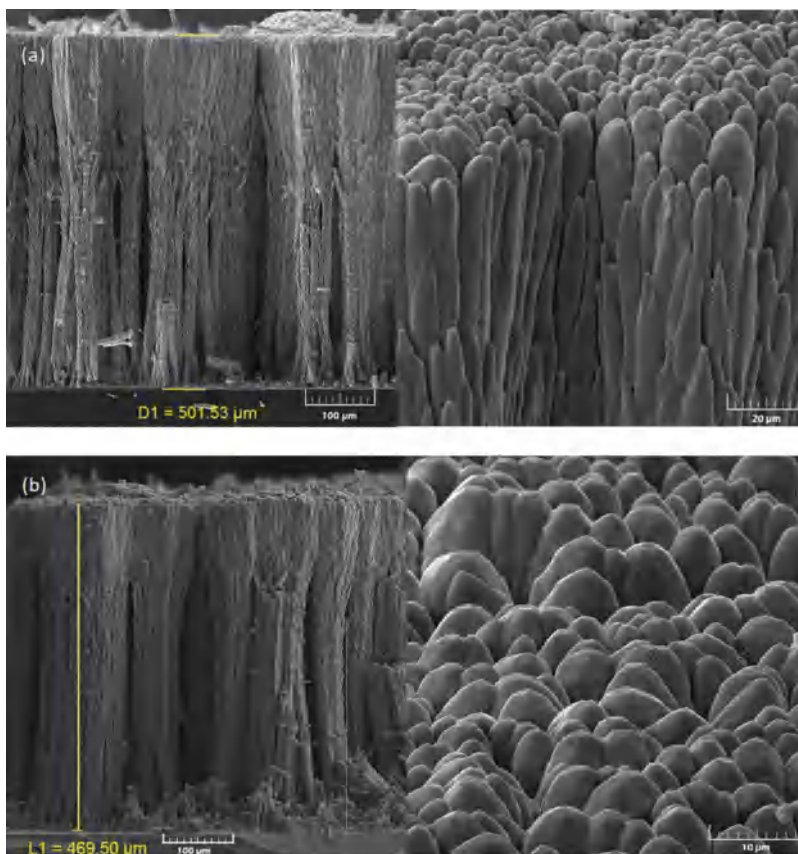


Fig. 2. Cross-sectional SEM images of (a) CsI(Na) and (b) CsI(Na, Eu) films.

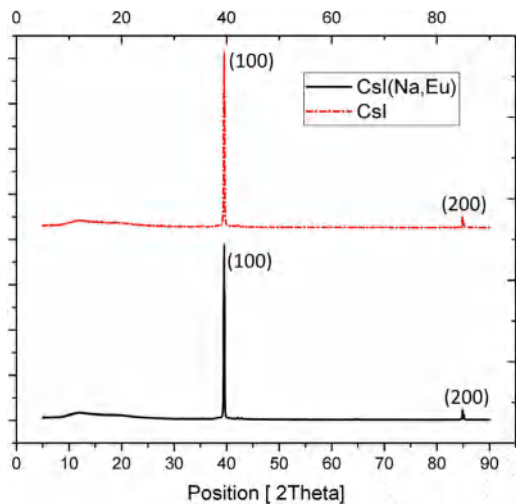


Fig. 3. X-ray diffraction patterns of CsI (dashed line) and CsI(Na, Eu) (solid line) films.

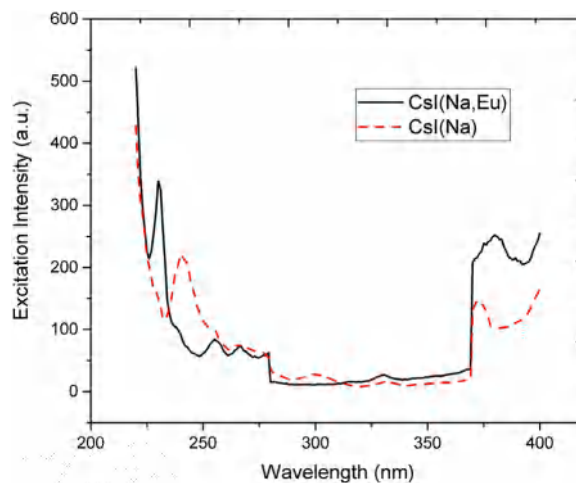


Fig. 4. The excitation spectrum of CsI(Na) (dashed line) and CsI(Na, Eu) (solid line) films at 430 nm.

The optical band gaps can be calculated according to the absorption spectrum, using the Tauc method [26], as shown in the inset of Fig. 6. The main band gaps of 3.1 eV for CsI(Na, Eu) and 2.95 eV for CsI(Na) film were obtained in the energy band range of 2–5 eV via analyzing Fig. 6 in Origin Pro software. By co-doping Eu and Na to CsI, it could be seen an increase in the number of available states with almost the same absorption gap of energy ( $\approx 3.18$  eV) in the region of 3.5–4.75 eV in Fig. 6, hence the absorption intensity is enhanced.

### 3.4. Photoluminescence

The excitation and PL spectrum were measured at  $90^\circ$  from the edge of film to decrease the interference from the reflected and transmitted light. The experimental setup has been illustrated in Fig. 7.

There is a slight hump in both thick films of CsI(Na) and CsI(Na, Eu) UV-emission spectra near 315 nm ( $\sim 3.9$  eV) in Fig. 8, which was intensified and seen better at a low temperature. It was known as an intrinsic band of pure CsI bulk crystal [10]. By doping, with  $\text{Na}^+$  replacing  $\text{Cs}^+$ , its higher electronegativity as well as its smaller

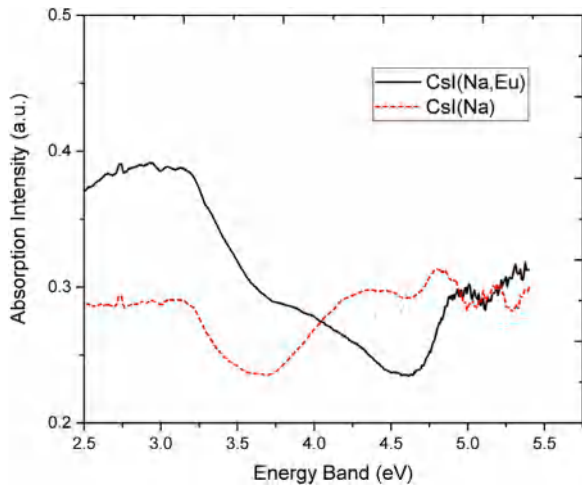


Fig. 5. UV absorption spectrum of CsI(Na) (dashed line) and CsI(Na, Eu) (solid line) films.

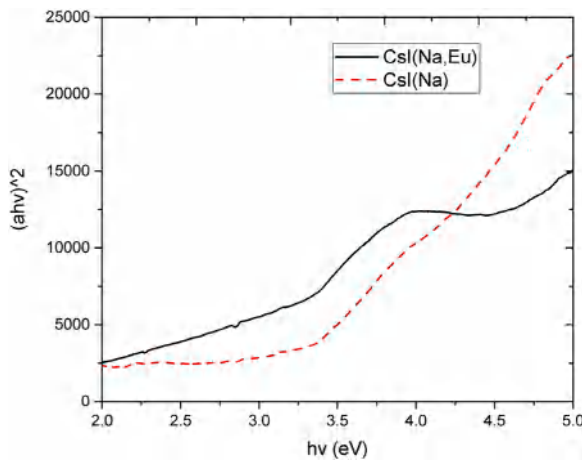


Fig. 6. Plotting graph of  $((ah\nu)^2)$  for CsI(Na) (dashed line) and CsI(Na, Eu) (solid line) absorption spectrum.

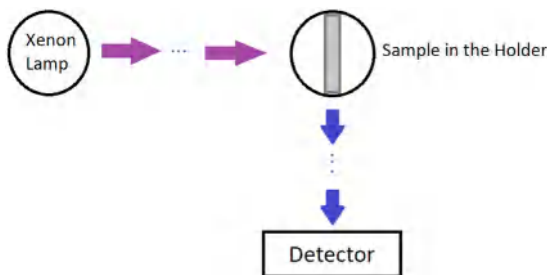


Fig. 7. Excitation and luminescence measuring setup.

size made perturbation in the lattice. The spectrum indicates a wide emission band in CsI(Na) with the main peak near the 435.3 nm, in its center that coincides with the blue emission at 420 nm in CsI(Na) bulk crystal, which was known as a characteristic of Na<sup>+</sup>-activated CsI (extrinsic band). Configuration of a self-trapped hole (STH) ( $V_k$ -center) near substitutional Na<sup>+</sup> in CsI is the main reason for the blue emission, which has been studied in CsI(Na) bulk crystal by Monnier et al. [4]. As a matter of fact, in comparison to bulk crystal, the thickness effect is a possible reason for an emission wavelength shift and the broadening of the CsI(Na) film.

The emission of CsI(Na, Eu) film in the region of 427.5 nm has a little shift as compared with CsI(Na). Moreover, there is a significant

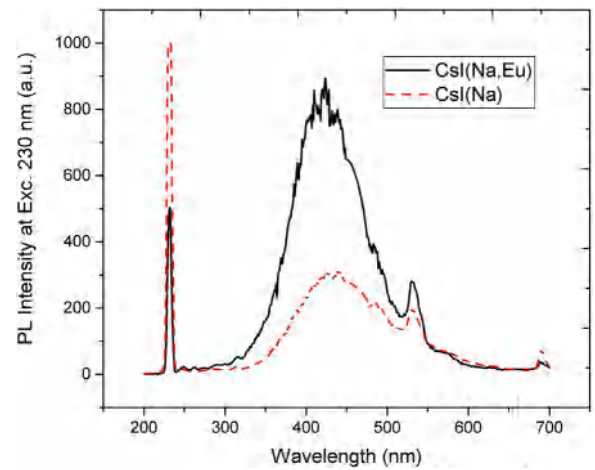
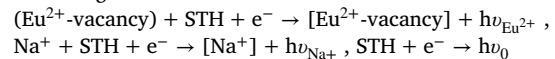


Fig. 8. Luminescence peak of CsI(Na) (dashed line) at 435.3 nm and CsI(Na, Eu) (solid line) at 427.5 nm (Ex. 230 nm).

enhancement in UV luminescence intensity of the CsI(Na, Eu) film, which confirmed the creation of additional centers as a result of the Eu doping into CsI(Na) film. Therefore, the luminescence properties of CsI(Na) columns differ from those of CsI(Na, Eu).

The addition of sensitizer has new effects (in addition to activator) on the crystal field because of the approach of the perturbation on the lattice. Divalent Eu<sup>2+</sup> substituted for the monovalent Cs<sup>+</sup>, accompanied by a vacancy as a charge compensator and vacancy-Eu<sup>2+</sup> dipole is formed. The differences in the radii of Cs<sup>+</sup> and Eu<sup>2+</sup> ions (~ 28%) [16] can also lead to a new lattice distortion. Co-doping of CsI perturbed the crystal field by complex formation of exciton, activator and sensitizer during excitation in the (CsI, NaI, EuI<sub>2</sub>) ternary system. The recombination energy for Na and Eu-localized in the host lattice can be described in the following form:



Energy is released in the lattice by a recombination of captured electron and  $V_k$ -center (STH) on Na<sup>+</sup> and Eu<sup>2+</sup>-vacancies, and a recombination of the captured electron and  $V_k$ -center (STH) of intrinsic band of pure CsI.

In this research, for the 500  $\mu\text{m}$  film with respect to co-doping (0.02% mol Na) and (0.001% mol Eu) concentration, there are an estimated number of 250 activator ions (Na) and about 10–12 sensitizer ions (Eu) in a row. So it is expected to have an intensive emission from Na centers, but a weak emission from Eu ones. As a result, Eu centers seem to have no significant effect on emission wavelength shift or intensity but this is in contradiction with what is illustrated in the PL spectrum of CsI(Na, Eu), CsI(Na) films at RT at exc. 230 nm in Fig. 9.

In this regard, it can be justified using another approach. In the other approach, there is an interaction between Na and Eu at RT. The energy transfer between a sensitizer and an activator occurs if a suitable interaction and energy difference between both systems exist. The exchange interaction is a part of this interaction; therefore, the resulting transfer is proportional to  $\int g_S(E) g_A(E) dE$  [27], which represents the spectral overlap, depending on exchange interaction between Eu and Na, as seen in Fig. 8. With attention to the luminescence intensity of Eu and Na, it is perceived that there is a high spectral overlap between absorption transition of Na  $\rightarrow$  Na\* (with normalized function  $g_{\text{Na}}(E)$ ) and emission transition of Eu\*  $\rightarrow$  Eu (with normalized function  $g_{\text{Eu}}(E)$ ); so, resonance condition will occur. It seems that in addition to Eu high quantum efficiency, the incorporation of Eu by interaction with Na and their high spectral overlap represent new channels for recombination in the region of 430 nm, which increases the blue luminescence intensity. It most likely has a direct impact on the improvement of scintillation light yielded by collecting and recognizing more photons.

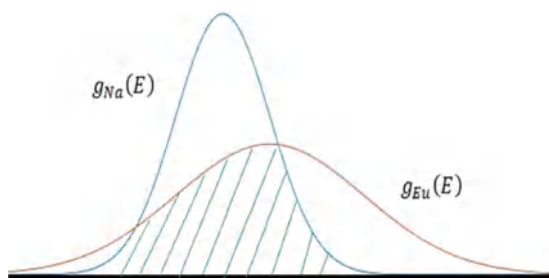


Fig. 9. Spectral overlap of Na and Eu doped CsI.

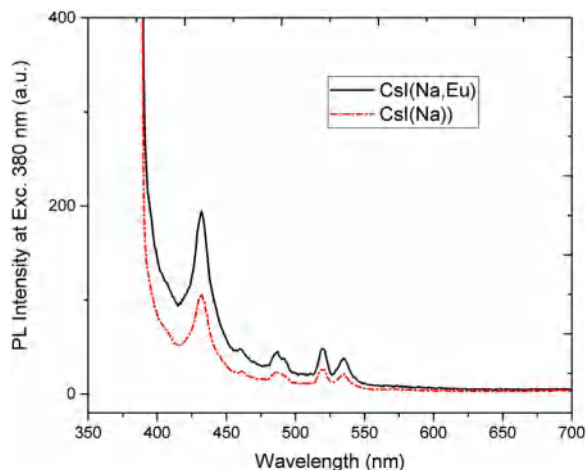


Fig. 10. Luminescence peak of CsI(Na) (dashed line) and CsI(Na, Eu) (solid line) films at 432 nm (Ex. 380 nm).

It should be mentioned that the small peaks in the luminescence spectra of CsI(Na) and CsI(Na, Eu) in Fig. 8 at 520 nm is probably related to the emission of the undesirable accumulation of Na nanoparticles, during the thick film deposition. With an increase in the excitation wavelength from 230 nm in both thick films, luminescence was turned off near 270 nm but again in the region of 370–400 nm it appeared and was heightened at exc. 380 nm, as seen in Fig. 9; but it was less intense than before because the luminescence and excitation in this region overlap and re-absorbance occurs. As seen in Fig. 10, the luminescence wavelength is measured at 432 nm.

### 3.5. Ionoluminescence

The IBIL of the prepared films was investigated via proton beam of 2.5 MeV and  $\sim 100$  pA current, with a spot size of  $10 \times 10 \mu\text{m}^2$  on the sample surface, and presented in Fig. 11. The intrinsic bands, which are characteristic of pure crystals, were lost because of high temperature in this surface spot. The existing peaks in CsI(Na) as seen in Fig. 11, in the region of 443 and 488 nm, probably indicate the activator defect, and two peaks near 435 and 483 nm and their higher intensities for CsI(Na, Eu) are associated with the occurrence of energy transfer. Owing to the high temperature produced during the test, the emergence of new peaks and a red wavelength shift can be attributed to phonon effects. These results verify the photoluminescence data.

Furthermore, the IBIL images of the samples were captured by CCD. Fig. 12 clarifies that CsI(Na, Eu) has better resolution than CsI(Na). Different color areas are the luminescence characteristics of the deposited films. An enhancement in the blue band width and its better resolution in CsI(Na, Eu) film as compared with CsI(Na) is results of the adding Eu as a sensitizer.

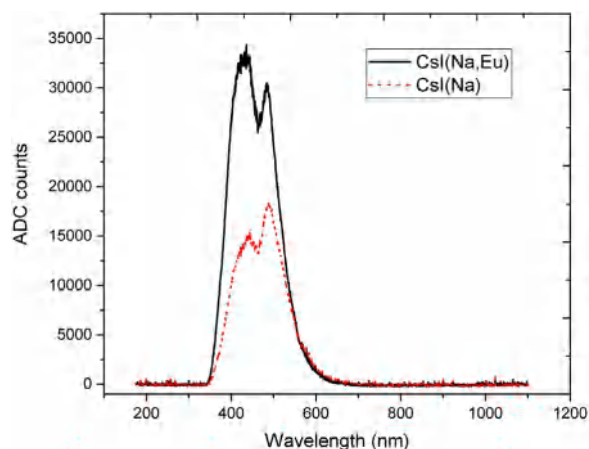


Fig. 11. IBIL spectra of CsI(Na) (dashed line) and CsI(Na, Eu) (solid line) layers.

### 3.6. Pulse height spectrum

The energy spectra of 661.6 keV  $\gamma$ -rays from a  $^{137}\text{Cs}$  source (20  $\mu\text{Ci}$ ), was obtained with the same dimensions of  $1'' \times 1'' \times 500 \mu\text{m}$  CsI(Na) and CsI(Na, Eu) thick films, was displayed in Fig. 13. The light yield (LY) and energy resolution,  $\Delta E/E$ , of the full energy peak for Cs  $\gamma$ -peak with a scintillator coupled to a photomultiplier tube, were measured by the method of comparison [28]. The CsI(Na, Eu) energy resolution was evaluated 12.59% and the value of 12.21% was obtained with CsI(Na). It should be noted that in spite of the comparable energy resolution of the films, there is a better photoelectron yield for CsI(Na, Eu) which is about 10% more than CsI(Na). The studies of tested CsI(Na) and CsI(Na, Eu) samples are summarized in Table 1, and NaI(Tl) light yield (100%) is taken as the reference [29].

As a result, in the case of energy transfer by co-doping activator and sensitizer to CsI,  $\text{Na}^+$  ion is excited to a metastable level  $E_1$  after excitation, if  $\text{Eu}^{2+}$  ion has high absorption in this excited bandwidth and also high fluorescence (high emission quantum yield) from a level lying close to  $E_1$ , it will accept part or all of the excitation energy deposited on  $E_1$ , consequently, emission from activator will be enhanced, the Eu sensitizer creates new recombination centers, so more scintillation photons were detected. It is essential to mention that, the undesirable increase in energy resolution is possible to origin from inhomogeneities in the deposited layer thickness, located in the PVD chamber statistically or inhomogeneities in  $\text{Eu}^{2+}$  impurity distribution and its associated defects in CsI(Na).

## 4. Conclusion

CsI(Na) and CsI(Na, Eu) films were deposited on the  $\text{TiO}_2$  coated quartz substrate by thermal evaporation, from the crushed single crystals as raw materials. The films' impurity concentration was measured by ICP-optical emission spectroscopy and the obtained data proved their close to that of raw materials. The SEM results showed a columnar structure, which is useful to capture and recognize photons. The surface morphology and structure of films are not affected by the addition of new impurities. It should be noted that the absorption and luminescence properties of these columns are changed by co-doping. Considering energy transfer – i.e. exchange interaction between Eu as a sensitizer and Na as an activator – it was observed a high-spectral overlap between absorption transition of Na and emission transition of Eu, which enhanced the blue luminescence intensity. In fact, the emergence of these new recombination centers along with the Eu high quantum efficiency, relying on its  $4f^6 5d \rightarrow 4f^7$  transitions, have a direct role in increasing the luminescence band. The IBIL results and their microscopic images confirmed the obtained photoluminescence data. The response

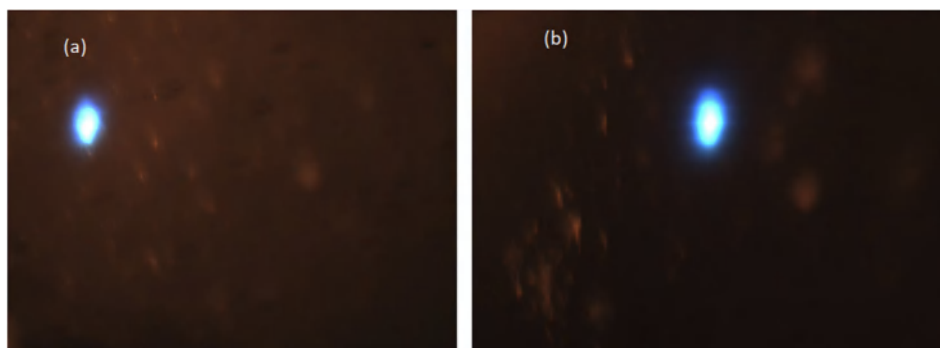


Fig. 12. The microscopic IBIL images of (a) CsI(Na) and (b) CsI(Na, Eu) films were captured by CCD.

Table 1  
Characteristics of CsI(Na) and CsI(Na, Eu) scintillators.

	Na (mol%)	Eu (mol%)	Emission wavelength (nm)	Light yield (LY%)	Energy resolution $\Delta E/E$ (%)
CsI(Na)	0.02	–	435	85	12.21
CsI(Na, Eu)	0.02	0.001	427	95	12.59

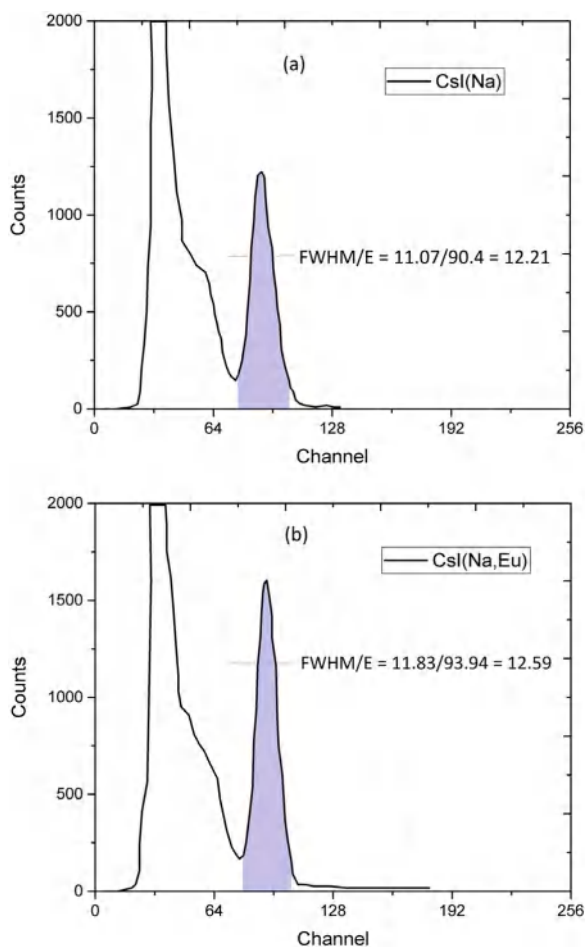


Fig. 13. Pulse height obtained for gamma radiation from  $^{137}\text{Cs}$  source with (a) CsI(Na) and (b) CsI(Na, Eu) thick films.

to  $^{137}\text{Cs}$  gamma rays verifies that the scintillation efficiency of CsI(Na) traditional film is improved by Eu co-doping. CsI(Na, Eu) light yield enhancement up to 10%, may have a direct impact on reducing the exposure of patients to the harmful radiation in medical imaging.

## Acknowledgments

We are indebted to Heidar Faripour for his valuable contributions in preparing the deposited films. We would like to thank Dr. Mustafa Aghazadeh for language corrections.

## References

- [1] G. Hrehuss, Scintillation response function and decay time of CsI(Na) to charged particles, *Nucl. Instrum. Methods* 68 (1969) 9.
- [2] C. Hsu, Olive Lee, W. Bates Jr, Absorption and emission due to localized excitons in CsI:Na, *J. Lumin.* 15 (1977) 75.
- [3] O.L. Hsu, Luminescence phenomena in CsI(Na), *J. Lumin.* 11 (1975) 65.
- [4] C.K. Ongt, K.S. Song, R. Monnier, A.M. Stoneham, Electronic structure and luminescence of CsI : Na, *J. Phys. C: Solid State Phys.* 12 (1979).
- [5] A. Syntfeld-Kauch, P. Siczynski, M. Moszynski, A.V. Gektin, W. Czarnacki, M. Grodzicka, J. Iwanowska, M. Szawłowski, T. Szczśniak, Świdzki, Energy resolution of CsI(Na) scintillators, *Radiat. Meas.* 45 (2010) 377.
- [6] D.W. Aitken, B.L. Beron, G. Yenicy, H.R. Zulliger, The fluorescent response of NaI(Tl), CsI(Tl), CsI(Na) and CaF<sub>2</sub>(Eu) to x-rays and low energy gamma rays, *IEEE Trans. Nucl. Sci.* 14 (1967) 468.
- [7] W. Bates, Scintillation processes in thin films of CsI(Na) and CsI(Tl) due to low energy x-rays, electrons and protons, *Adv. Electron. Electron Phys.* 28 (1969) 451.
- [8] E.A. Kozyrev, K.E. Kuper, A.G. Lemzyakov, A.V. Petrozhitskiy, A.S. Popov, X-ray tomography using thin scintillator films, in: *Cern Proc., CERN in Geneva, 2017*, p. 22.
- [9] F. Liu, X. Ouyang, M. Tang, Y. Xiao, B. Liu, X. Zhang, Y. Feng, J. Zhang, J. Liu, Scaling-induced enhancement of x-ray luminescence in CsI(Na) crystals, *Appl. Phys. Lett.* 102 (2013) 181107.
- [10] M. Nakayama, N. Ando, J. Hirai, H. Nishimura, Scintillation activated by nanoparticle formation in CsI:Na thin films, *J. Lumin.* 108 (2004) 359.
- [11] Y. Wu, G. Ren, F. Meng, X. Chen, D. Ding, H. Li, Ultralow-concentration Sm codoping in CsI : Tl scintillator: A case of little things can make a big difference, *Opt. Mater. (Amst)* 38 (2014) 297.
- [12] D. Totsuka, T. Yanagida, Y. Fujimoto, Y. Yokota, F. Moretti, A. Vedda, A. Yoshikawa, Afterglow suppression by codoping with Bi in CsI:Tl crystal scintillator, *Appl. Phys. Express* 5 (2012) 052601-1.
- [13] N.V. Shiran, A.V. Gektin, Y. Boyarintseva, S. Vasyukov, A. Boyarintsev, V. Pedash, S. Tkachenko, O. Zelenskaya, N. Kosinov, O. Kisel, L. Philippovich, Eu doped and Eu, Tl co-doped NaI scintillators, *IEEE Trans. Nucl. Sci.* 57 (2010) 1233.
- [14] L.A. Kappers, R.H. Bartram, D.S. Hamilton, A. Lempicki, C. Brecher, V. Gaysinskiy, E.E. Ovechkina, S. Thacker, V.V. Nagarkar, A tunneling model for afterglow suppression in CsI : Tl, Sm scintillation materials, *Radiat. Meas.* 45 (2010) 426.
- [15] C. Brecher, A. Lempicki, S.R. Miller, J. Glodo, E.E. Ovechkina, Suppression of afterglow in CsI : Tl by codoping with Eu 2+ — I : Experimental, *Nucl. Instrum. Methods Phys. Res.* 558 (2006) 450.
- [16] A.M. Lebedynskiy, N.V. Shiran, A.V. Gektin, A.G. Fedorov, Structure and columnar films of CsI : Eu columnar films, *Appl. Spectrosc.* 79 (2012) 599.
- [17] H.J. Seo, W.S. Zhang, T. Tsuboi, S.H. Doh, W.G. Lee, H.D. Kang, K.W. Jang, Luminescence properties of a CsI crystal doped with Eu 2+ ions, *Alloy. Compd.* 344 (2002) 268.

- [18] A. Gektin, N. Shiran, A. Belsky, S. Vasyukov, Luminescence properties of CsI : Eu crystals, *Opt. Mater. (Amst)* 34 (2017) 2017.
- [19] A. Gektin, N. Shiran, A. Belsky, A. Vasil'ev, Luminescence fundamental limits for alkali halide scintillators, in: 3d SUCCESS Int. Sci. Work, 2012, pp. 66–67.
- [20] H.R.K.H. Frey, *Handbook of Thin Film Technology*, 2015.
- [21] V. Yakovlev, L. Trefilova, A. Meleshko, Y. Ganja, Short-living absorption and emission of CsI(Na), *J. Lumin.* 131 (2011) 2579.
- [22] G.F. Knoll, Scintillation detector, in: *Introd. to Radiat. Detect. Meas.*, 1998, p. 20.
- [23] V.V. Nagarkar, V. Gaysinskiy, E.E. Ovechkina, S.C. Thacker, S.R. Miller, C. Brecher, A. Lempicki, Suppression of afterglow in CsI(Tl) by codoping with Eu<sup>2+</sup>: Fabrication of microcolumnar films for high-resolution high-speed imaging, *IEEE Trans. Nucl. Sci.* 54 (2007) 1378.
- [24] C.W.E. Van Eijk, Inorganic scintillators in medical imaging detectors, *Phys. Med. Biol.* 47 (2002) R99.
- [25] M. Overdick, Detectors for x-ray imaging and computed tomography, in: *Adv. Healthc. Technol. Shap. Futur. Med. Care*, 2006, pp. 49–64.
- [26] A. Tumuluri, K.L. Naidu, K.C.J. Raju, Band gap determination using tauc 's plot for LiNbO<sub>3</sub> thin films, *Int. J. ChemTech Res.* 6 (2014) 3353–3356.
- [27] A.H. Kitai, Lamp phosphors, in: *Solid State Lumin.*, 1993, pp. 36–44.
- [28] E. Sysoeva, V. Tarasov, O. Zelenskaya, Comparison of the methods for determination of scintillation light yield, *Nucl. Instrum. Methods Phys. Res. A* 486 (2002) 67–73.
- [29] N. Tsoufanidis, S. Landsberger, *Measurement and detection of radiation*, fourth ed., 486, CRC Press Taylor & Francis Group, 2015, p. 200.